



Cite this: *Dalton Trans.*, 2022, **51**, 8945


Received 12th May 2022,

Accepted 18th May 2022

DOI: 10.1039/d2dt01477g

rsc.li/dalton

An $[\text{Fe}^{\text{III}}_8]$ molecular oxyhydroxide†

Daniel J. Cutler, ^a Marco Coletta, ^a Mukesh K. Singh, ^a Angelos B. Canaj, ^a Laura J. McCormick, ^b Simon J. Coles, ^b Jürgen Schnack ^{*c} and Euan K. Brechin ^{★a}

An $[\text{Fe}^{\text{III}}_8]$ hexagonal bipyramid displays antiferromagnetic exchange between the two capping tetrahedral ions and the six ring octahedral ions resulting in a spin ground state of $S = 10$.

Polymetallic complexes of Fe^{III} ions have always played a prominent role in the development molecular magnetism. $[\text{Fe}^{\text{III}}_2]$ dimers,¹ $[\text{Fe}^{\text{III}}_3]$ triangles² and $[\text{Fe}^{\text{III}}_4]$ butterflies³ not only represented ideal systems for developing quantitative magneto-structural correlations, they were also employed synthetically as starting materials for constructing larger and more complex species.⁴ The latter often contain the same vertex-, edge-, face-sharing structural units as the reactants, linked *via* organic and inorganic bridging ligands. The large library of complexes produced therefrom allowed chemists to understand the processes by which larger clusters self-assemble, allowing some control over the resultant magnetic properties, targeting, for example, slow relaxation of the magnetisation,⁵ spin frustration,⁶ or an enhanced magnetocaloric effect.⁷

One interesting sub-set of species in this family are molecular iron oxides, an emerging class of materials whose structures, in the main, contain no bridging organic ligands and conform to mineral phases such as ferrihydrite and magnetite.⁸ As well as displaying fascinating magnetic behaviours, such species potentially have applications in a breadth of areas ranging from catalysis⁹ and battery technologies¹⁰ to biomedical imaging.¹¹

The striking structural similarities between the molecular iron oxides $[\text{Fe}^{\text{III}}_{13}]$,¹² $[\text{Fe}^{\text{III}}_{17}]$,^{8,13} $[\text{Fe}^{\text{III}}_{30}]$,¹⁴ and $[\text{Fe}^{\text{III}}_{34}]$ ¹⁵

which all possess alternating “layers” or tetrahedral and octahedral Fe^{III} ions has prompted us to speculate, and examine, whether very large molecular iron oxides, perhaps even rivaling the size and complexity of the polyoxometalates,¹⁶ can be isolated. The inability of Fe^{III} to be stabilised by terminal oxide ions and the propensity of aqueous solutions of Fe^{III} to produce mixtures of intractable/insoluble/amorphous solids suggests however that alternative synthetic pathways may have to be explored. The simplicity of the synthesis of $[\text{Fe}_{17}]$ represents a good starting point. It is made by dissolving anhydrous FeBr_3 in wet pyridine.^{8,13} The latter acts as solvent, base, source of oxide/hydroxide, terminal ligand and charge balancing counter cation (pyH^+). Analogous reactions replacing the pyridine with β -picoline, 4-ethylpyridine, isoquinoline, 3,4-lutidine, results in a series of isostructural species.¹³ Addition of different bases, templates and solvent combinations results in the formation of the related, but larger $[\text{Fe}_{30}]$ and $[\text{Fe}_{34}]$ clusters.^{14,15} Herein, we extend this methodology to the use of 4-methoxypyridine (MeO-py) and the synthesis of the smallest member of this molecular iron oxide family, an $[\text{Fe}_8]$ cage.

Dissolution of FeBr_3 in MeO-py with stirring for 2.5 hours, followed by filtration and vapour diffusion with acetone results in the formation of orange plate-like crystals in 2 weeks. Crystals of $[\text{Fe}^{\text{III}}_8\text{O}_6(\mu\text{-OH})_6(\text{MeO-py})_{12}\text{Br}_2]\text{Br}_4 \cdot 3\text{H}_2\text{O} \cdot 2\text{MeO-py}$ ($1 \cdot 3\text{H}_2\text{O} \cdot 2\text{MeO-py}$; Fig. 1) are in a monoclinic crystal system and structure solution was performed in the space group $C2/c$ (Table S1 and Fig. S1†). The asymmetric unit contains half the formula. The metallic skeleton of **1** describes a hexagonal bipyramid, in which a ring of six octahedral Fe^{III} ions (Fe1–3 and symmetry equivalent, s.e.) is capped top and bottom by a tetrahedral Fe^{III} ion (Fe4 and s.e.). The tetrahedral Fe^{III} ions are linked to the $[\text{Fe}_6]$ ring through three $\mu_3\text{-O}^{2-}$ ions (O10, O20, O30 and s.e.), which further bridge two octahedral Fe ions around the inner rim of the wheel. The outer rim is bridged by six $\mu\text{-OH}^-$ ions (O1H, O2H, O3H and s.e.). The coordination sphere of the tetrahedral Fe ion is completed by the presence of a terminal Br^- ion (Br3 and s.e.), and those of the octahedral Fe ions by two MeO-py molecules. Fe–O–Fe

^aEastCHEM School of Chemistry, The University of Edinburgh, David Brewster Road, Edinburgh, EH9 3FJ Scotland, UK. E-mail: E.Brechin@ed.ac.uk

^bEPSRC National Crystallography Service, School of Chemistry, University of Southampton, Highfield, Southampton, SO17 1BJ, UK

^cUniversität Bielefeld, Postfach 100131, D-33501 Bielefeld, Germany. E-mail: jschnack@uni-bielefeld.de

†Electronic supplementary information (ESI) available: Details of methods and materials, physical characterisation data, computational details. CCDC 2163355. For ESI and crystallographic data in CIF or other electronic format see DOI: <https://doi.org/10.1039/d2dt01477g>

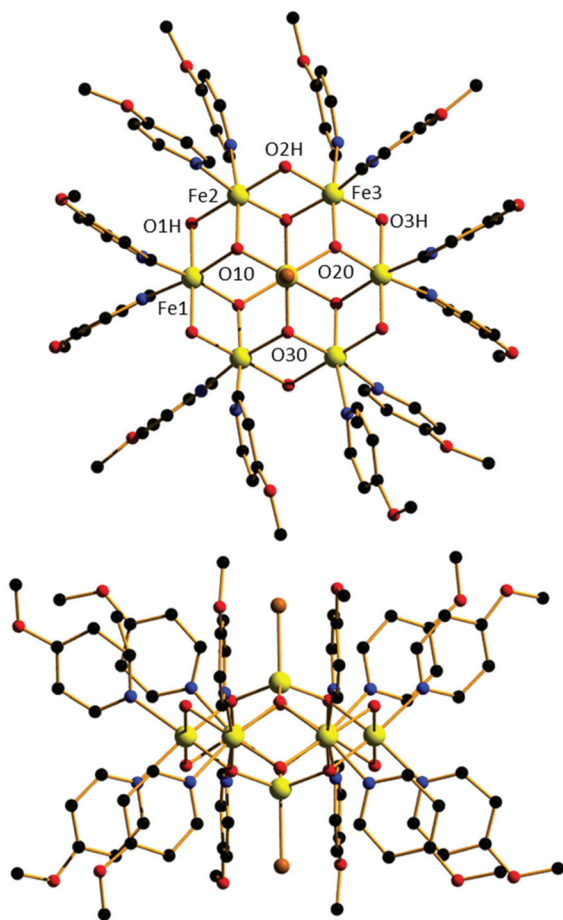


Fig. 1 Orthogonal views of the molecular structure of the cation of **1**. Colour code: Fe = yellow, O = red, N = blue, Br = brown, C = black. H atoms, counter anions and solvent of crystallisation omitted for clarity.

bond angles fall in the ranges Fe(tet)–O–Fe(oct), 122.62–123.42°, and Fe(oct)–O–Fe(oct), 95.25–98.38°; note that the former are very much bigger than the latter. The Br[−] counter anions (Br1, Br2 and s.e.) are H-bonded to the μ -OH ions (Br \cdots O, 3.199–3.227 Å), as are the two MeO-py and three H₂O molecules of crystallization (Br \cdots O, 3.365–3.674 Å; N \cdots O, 2.847 Å; Fig. S2†). Closest inter-cluster interactions are between neighbouring MeO-py molecules at C/O \cdots C/O distances \geq 3.45 Å (Fig. S3†). The structural similarity between **1** and [Fe₁₇] can be seen in Fig. 2 in which the [Fe₈] cation can be directly mapped onto half of the [Fe₁₇] framework. The similarity between [Fe₈] and [Fe₁₃], [Fe₁₇], [Fe₃₀], [Fe₃₄] and selected Fe minerals is shown in Fig. S4.† The hexagonal bipyramidal core is unique amongst the [Fe₈] clusters reported in the Cambridge Structural Database, but the same unit exists in two [Fe₁₄] clusters, [Fe₁₄(bta)₆O₆(OMe)₁₈Cl₆] (where btaH = 1,2,3-benzotriazole) and [Gd₁₂Fe₁₄O₁₂(OH)₁₈(tea)₆(CH₃COO)₁₆(H₂O)₈] (where H₃tea = triethanolamine), whose Fe metallic skeletons both describe hexacapped hexagonal bipyramids, albeit with the Fe ions all being octahedral.^{7,17} Complex **1** also has some structural simi-

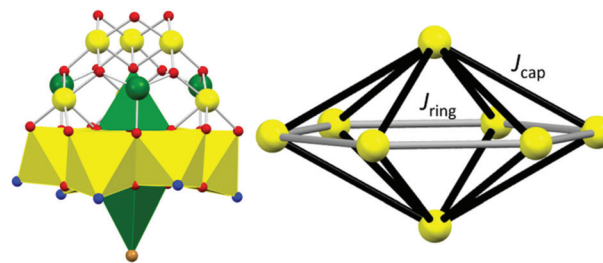


Fig. 2 The structure of [Fe₈] in polyhedral format mapped onto half of the [Fe₁₇] cluster represented in ball and stick format (left). The magnetic skeleton of **1** highlighting the two magnetic exchange interactions, J_{cap} and J_{ring} (right).

ilarity to a family of [Fe₇] clusters whose metallic skeletons describe a capped hexagon or ‘dome-like’ topology. Magnetic measurements of these species suggested the presence of significant spin frustration effects.¹⁸

Magnetic measurements of **1** reveal strong, dominant anti-ferromagnetic interactions between the Fe^{III} ions. The experimental dc susceptibility data ($T = 2$ –300 K, $B = 0.1$ T) for **1** are plotted in Fig. 3 as the χT product versus T , where χ is the

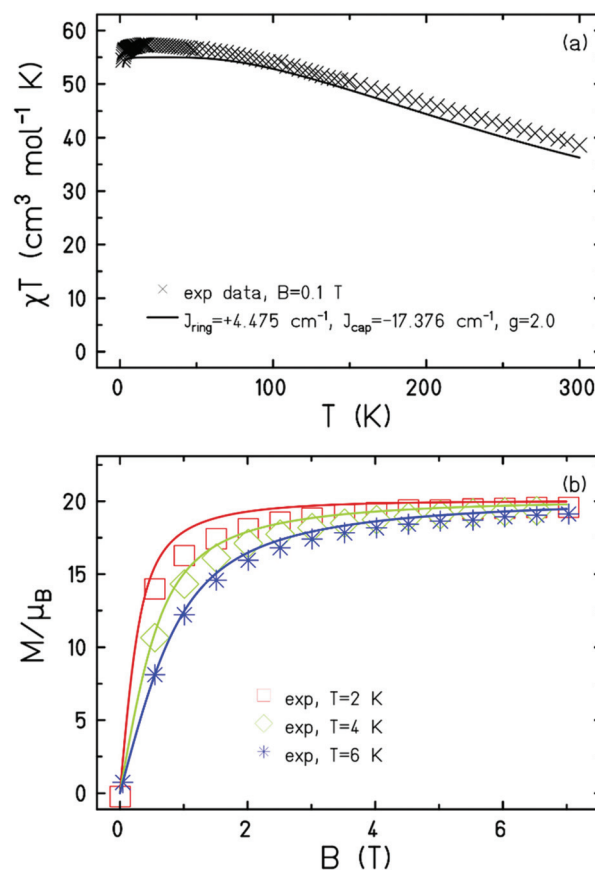


Fig. 3 (a) Plot of the χT product versus T in the 300–2 K temperature range in an applied field, $B = 0.1$ T. (b) Plot of M versus B in the 2–7 K range for $0.5 \leq B \leq 7$ T. The solid lines represent a fit of the experimental data with the indicated parameters. See text for details.



molar magnetic susceptibility, T is the temperature, and B the field. The value of χT at $T = 300$ K is $\sim 38 \text{ cm}^3 \text{ K mol}^{-1}$, larger than that expected for the sum of the Curie constants for eight Fe^{III} ($S = 5/2$) ions with $g_{\text{Fe}} = 2.00$ ($35 \text{ cm}^3 \text{ K mol}^{-1}$). As the temperature decreases, the magnitude of χT increases rapidly, reaching a maximum value of $\sim 57 \text{ cm}^3 \text{ K mol}^{-1}$ at $T = 16$ K, where it then plateaus before decreasing slightly to a value of $\sim 55 \text{ cm}^3 \text{ K mol}^{-1}$ at $T = 2$ K. The data are clearly indicative of competing ferro- and antiferromagnetic interactions, with the maximum in χT suggesting a ground state spin value of $S = 10$. This is corroborated by magnetisation data ($T = 2\text{--}7$ K, $B = 0.5\text{--}7$ T; Fig. 3) which rise rapidly with increasing field strength and saturate just below $M = 20 \mu_{\text{B}}$. Given the large discrepancy in the $\text{Fe}(\text{tet})\text{--O--Fe}(\text{oct})$ and $\text{Fe}(\text{oct})\text{--O--Fe}(\text{oct})$ bond angles, the data suggest a strong antiferromagnetic interaction between the tetrahedral and octahedral Fe ions, analogous to that seen for $[\text{Fe}_{17}]$,^{8,13} and consistent with published magneto-structural studies of O-bridged Fe^{III} compounds.¹ The magnetic data can be simulated using exact diagonalisation¹⁹ and an isotropic spin-Hamiltonian $\hat{H} = -2 \sum_{i < j} J_{ij} \hat{s}_i \cdot \hat{s}_j$

with a coupling scheme that assumes just two independent exchange interactions, J_{ring} and J_{cap} , describing the interaction between the octahedral ions in the $[\text{Fe}_6]$ wheel and between the tetrahedral and octahedral Fe ions, respectively (Fig. 3). This affords $J_{\text{ring}} = +4.475 \text{ cm}^{-1}$ and $J_{\text{cap}} = -17.376 \text{ cm}^{-1}$ with $g = 2.00$. This results in a spin ground state of $S = 10$.

To further support the relative sign and magnitude of the exchange interactions obtained experimentally, we have performed DFT calculations on both dimeric and trimeric models derived from the full structure of **1** (Fig. S6 and 7; see ESI† for computational details).²⁰ This affords $J_{\text{ring}} = +4.1 \text{ cm}^{-1}$ and $J_{\text{cap}} = -30.1 \text{ cm}^{-1}$ for the dimeric model, and $J_{\text{ring}} = +2.1 \text{ cm}^{-1}$ and $J_{\text{cap}} = -30.4 \text{ cm}^{-1}$ for the trimeric model. We have also performed overlap integral calculations between the singly occupied molecular orbitals of the Fe^{III} ions.^{20,21} These suggest three moderate magnetic orbital overlaps for J_{ring} resulting in small ferromagnetic interactions (Table S2 and Fig. S8a–c†), and one strong and ten moderate magnetic orbital overlaps for J_{cap} leading to strong antiferromagnetic interactions (Table S2 and Fig. S8d–n†). Spin density analysis indicates the presence of a strong spin delocalization mechanism, as seen previously for other polymetallic iron complexes (Fig. S9†).²⁰

In conclusion, the simple reaction between anhydrous FeBr_3 and MeO-py results in the formation of an $[\text{Fe}^{\text{III}}_8]$ cluster whose metallic skeleton conforms to a hexagonal bipyramid. Magnetic measurements reveal antiferromagnetic exchange between the two capping tetrahedral Fe^{III} ions and the six ring octahedral Fe^{III} ions leading to an $S = 10$ ground state. While the single capping Fe^{III} unit in the three $[\text{Fe}_7]$ systems was not sufficient to overcome the spin frustration and force the six spins in the ring parallel, the presence of two such caps in $[\text{Fe}_8]$, each strongly coupled to the six ring spins, has now overcome the frustration effects. The ease of synthesis and the striking structural similarity of $[\text{Fe}_8]$ to other molecular iron oxides such as $[\text{Fe}_{13}]$, $[\text{Fe}_{17}]$, $[\text{Fe}_{30}]$ and $[\text{Fe}_{34}]$ suggests that

many more such species with much larger nuclearities remain undiscovered.

Conflicts of interest

There are no conflicts to declare.

Acknowledgements

E. K. B. thanks the EPSRC (EP/V010573/1). M. K. S. would like to thank Edinburgh Compute and Data Facility (ECDF), and the European Union Horizon 2020 research and innovation programme under the Marie Skłodowska-Curie grant agreement no. 832488. For the purpose of open access, the author has applied a Creative Commons Attribution (CC BY) license to any Author Accepted Manuscript version arising from this submission.

Notes and references

- H. Weihe and H. U. Güdel, *J. Am. Chem. Soc.*, 1998, **120**, 2870–2879.
- R. D. Cannon and R. P. White, *Prog. Inorg. Chem.*, 1998, **36**, 195–298.
- J. K. McCusker, J. B. Vincent, E. A. Schmitt, M. L. Mino, K. Shin, D. K. Coggin, P. M. Hagen, J. C. Huffman, G. Christou and D. N. Hendrickson, *J. Am. Chem. Soc.*, 1991, **113**, 3012–3302.
- C. Cañada-Vilalta, T. A. O'Brien, E. K. Brechin, M. Pink, E. R. Davidson and G. Christou, *Inorg. Chem.*, 2004, **43**, 5505–5521.
- D. Gatteschi, R. Sessoli and A. Cornia, *Chem. Commun.*, 2000, 725–732.
- V. O. Garlea, S. E. Nagler, J. L. Zarestky, C. Stassis, D. Vaknin, P. Kögerler, D. F. McMorro, C. Niedermayer, D. A. Tennant, B. Lake, Y. Qiu, M. Exler, J. Schnack and M. Luban, *Phys. Rev. B: Condens. Matter Mater. Phys.*, 2006, **73**, 024414.
- (a) D. M. Low, L. F. Jones, A. Bell, E. K. Brechin, T. Mallah, E. Rivière, S. J. Teat and E. J. L. McInnes, *Angew. Chem., Int. Ed.*, 2013, **42**, 3781–3784; (b) R. Shaw, R. H. Laye, L. F. Jones, D. M. Low, C. Talbot-Eckelaers, Q. Wei, C. J. Milios, S. Teat, M. Helliwell, J. Raftery, M. Evangelisti, M. Affronte, D. Collison, E. K. Brechin and E. J. L. McInnes, *Inorg. Chem.*, 2007, **46**, 4968–4978; (c) E. Garlatti, S. Carretta, J. Schnack, G. Amoretti and P. Santini, *Appl. Phys. Lett.*, 2013, **103**, 202410.
- G. W. Powell, H. N. Lancashire, E. K. Brechin, D. Collison, S. L. Heath, T. Mallah and W. Wernsdorfer, *Angew. Chem., Int. Ed.*, 2004, **43**, 5772–5775.
- H. Docherty, J. Peng, A. P. Dominey and S. P. Thomas, *Nat. Chem.*, 2017, **9**, 595–600.
- C. Xie, Y. Duan, W. Xu, H. Zhang and X. Li, *Angew. Chem., Int. Ed.*, 2017, **56**, 14953–14957.



- 11 R. A. Revia and M. Zhang, *Mater. Today*, 2016, **19**, 157–168.
- 12 (a) A. Bino, M. Ardon, D. Lee, B. Spingler and S. J. Lippard, *J. Am. Chem. Soc.*, 2002, **124**, 4578–4579; (b) J. van Slageren, P. Rosa, A. Caneschi, R. Sessoli, H. Casellas, Y. V. Rakitin, L. Cianchi, F. Del Giallo, G. Spina, A. Bino, A.-L. Barra, T. Guidi, S. Carretta and R. Caciuffo, *Phys. Rev. B: Condens. Matter Mater. Phys.*, 2006, **73**, 014422; (c) O. Sadeghi, L. N. Zakharov and M. Nyman, *Science*, 2015, **347**, 1359–1362; (d) O. Sadeghi, C. Falaise, P. I. Molina, R. Hufschmid, C. F. Campana, B. C. Noll, N. D. Browning and M. Nyman, *Inorg. Chem.*, 2016, **55**, 11078–11088; (e) N. A. G. Bandeira, O. Sadeghi, T. J. Woods, Y.-Z. Zhang, J. Schnack, K. R. Dunbar, M. Nyman and C. Bo, *J. Phys. Chem. A*, 2017, **121**, 1310–1318.
- 13 (a) C. Vecchini, D. H. Ryan, L. M. D. Cranswick, M. Evangelisti, W. Kockelmann, P. G. Radaelli, A. Candini, M. Affronte, I. A. Gass, E. K. Brechin and O. Moze, *Phys. Rev. B: Condens. Matter Mater. Phys.*, 2008, **77**, 224403; (b) M. Evangelisti, A. Candini, A. Ghirri, M. Affronte, G. W. Powell, I. A. Gass, P. A. Wood, S. Parsons, E. K. Brechin, D. Collison and S. L. Heath, *Phys. Rev. Lett.*, 2006, **97**, 167202; (c) I. A. Gass, C. J. Milios, M. Evangelisti, S. L. Heath, D. Collison, S. Parsons and E. K. Brechin, *Polyhedron*, 2007, **26**, 1835–1837; (d) I. A. Gass, E. K. Brechin and M. Evangelisti, *Polyhedron*, 2013, **52**, 1177–1180.
- 14 A. E. Dearle, D. J. Cutler, M. Coletta, E. Lee, S. Dey, S. Sanz, H. W. L. Fraser, G. S. Nichol, G. Rajaraman, J. Schnack, L. Cronin and E. K. Brechin, *Chem. Commun.*, 2022, **58**, 52–22.
- 15 A. E. Dearle, D. J. Cutler, H. W. L. Fraser, S. Sanz, E. Lee, S. Dey, I. F. Diaz-Ortega, G. S. Nichol, H. Nojiri, M. Evangelisti, G. Rajaraman, J. Schnack, L. Cronin and E. K. Brechin, *Angew. Chem., Int. Ed.*, 2019, **58**, 16903–16906.
- 16 (a) M. T. Pope and A. Müller, *Angew. Chem., Int. Ed. Engl.*, 1991, **30**, 34–48; (b) H. N. Miras, J. Yan, D.-L. Liang and L. Cronin, *Chem. Soc. Rev.*, 2012, **41**, 7403–7430.
- 17 X.-Y. Zheng, H. Zhang, Z. Wang, P. Liu, M.-H. Du, Y.-Z. Han, R.-J. Wei, Z.-W. Ouyang, X.-J. Kong, G. i.-L. Zhuang, L.-S. Long and L.-S. Zheng, *Angew. Chem., Int. Ed.*, 2017, **56**, 11475–11479.
- 18 (a) L. F. Jones, P. Jensen, B. Moubaraki, K. J. Berry, J. F. Boas, J. R. Pilbrow and K. S. Murray, *J. Mater. Chem.*, 2006, **16**, 260–2697; (b) S. Mukherjee, R. Bagai, K. A. Abboud and G. Christou, *Inorg. Chem.*, 2011, **50**, 3489–3851; (c) K. C. Mondal, V. Mereacre, G. E. Kostakis, Y. Lan, C. E. Anson, I. Prisecaru, O. Waldmann and A. K. Powell, *Chem. – Eur. J.*, 2015, **21**, 10835–10842.
- 19 (a) K. Bärwinkel, H.-J. Schmidt and J. Schnack, *J. Magn. Magn. Mater.*, 2000, **212**, 240–250; (b) R. Schnalle and J. Schnack, *Int. Rev. Phys. Chem.*, 2010, **29**, 403–452; (c) T. Heitmann and J. Schnack, *Phys. Rev. B*, 2019, **99**, 134405.
- 20 (a) M. K. Singh and G. Rajaraman, *Inorg. Chem.*, 2019, **58**, 3175–3188; (b) D. J. Cutler, M. K. Singh, G. S. Nichol, M. Evangelisti, J. Schnack, L. Cronin and E. K. Brechin, *Chem. Commun.*, 2021, **57**, 8925–8928.
- 21 (a) M. Coletta, T. G. Tziotzi, M. Gray, G. S. Nichol, M. K. Singh, C. J. Milios and E. K. Brechin, *Chem. Commun.*, 2021, **57**, 4122–4125; (b) M. K. Singh, *Dalton Trans.*, 2020, **49**, 4539–4548; (c) M. Coletta, S. Sanz, D. J. Cutler, S. J. Teat, K. J. Gagnon, M. K. Singh, E. K. Brechin and S. J. Dalgarno, *Dalton Trans.*, 2020, **49**, 14790–14797; (d) M. K. Singh, T. Rajeshkumar, R. Kumar, S. K. Singh and G. Rajaraman, *Inorg. Chem.*, 2018, **57**, 1846–1858; (e) M. K. Singh, N. Yadav and G. Rajaraman, *Chem. Commun.*, 2015, **51**, 17732–17735.

